A Dinuclear Ruthenium Catalyst with Confined Cavity: Selectivity in the Addition of Aliphatic Carboxylic Acids to Phenylacetylene

Kwong-Chak Cheung, Wing-Leung Wong, Ming-Him So, Zhong-Yuan Zhou, Siu-Cheong Yan and Kwok-Yin Wong*

Department of Applied Biology and Chemical Technology, and The State Key Laboratory of Chirosciences, The Hong Kong Polytechnic University, Hunghom, Kowloon, Hong Kong, China.

E-mail: bckywong@polyu.edu.hk; Fax: +852 2364 9932; Tel: +852 3400 8686.

List of contents

(17) Figure S6. ^{13}C NMR spectrum of a reaction of mononuclear catalyst [(Ru(*p*-cymene)](CF_3SO_3)**DPPA**](CF_3SO_3) with phenylacetylene in CD_3OD.

(18) Figure S7. ^{13}C NMR spectrum of a reaction of dinuclear catalyst [(Ru(*p*-cymene)(CF_3SO_3))$_2$ **BDPAA**](CF_3SO_3)$_2$ with phenylacetylene in CD_3OD.

(19) Figure S8. ESI-MS of the reaction of active mononuclear catalyst [(Ru(*p*-cymene)](CF_3SO_3)**DPPA**](CF_3SO_3) with phenylacetylene.

(20) Figure S9. ESI-MS of the reaction of active dinuclear catalyst [(Ru(*p*-cymene)(CF_3SO_3))$_2$ **BDPAA**](CF_3SO_3)$_2$ with phenylacetylene.

(1) **Synthesis of 1,8-Diaminoanthraquinone**

A reaction mixture of 1,8-dichloroanthracene-9,10-dione (41.6 g, 0.15 mol), phthalimide (52.7 g, 0.385 mol) and anhydrous sodium acetate (29.6 g, 0.361 mol) in nitrobenzene (77 mL) was stirred and heated to 180 ^{o}C. After that, quinoline (25 mL) and copper powder (300 mesh, 0.72 g) were added to the reaction solution. The resulting mixture was heated at 200 ^{o}C for 1 h. The reaction mixture was allowed to cool down slowly and was then kept overnight without stirring under room temperature conditions. The precipitates were collected by filtration and washed sequentially with nitrobenzene (3 x 100 mL), ethanol (3 x 100 mL), hot water (2 x 100 mL), ethanol (2 x 100 mL), and ether (2 x 100 mL). After drying under vacuum, a crude diphthalimide intermediate was obtained as a pale yellowish orange solid (56.7 g, 76 %). The diphthalimide intermediate (56.0 g) was then reacted with concentrated H_2SO_4 (400 mL) with stirring at 95 ^{o}C for 45 min. The reaction mixture was cooled to 5 ^{o}C. To this solution crushed ice (150 g) was added slowly. The resulting mixture was poured into a beaker containing iced-water (1.5 L). The solution was stirred and the precipitates were collected by filtration. The collected solids were washed with water until the pH became neutral. After drying under vacuum, 1,8-diaminoanthraquinone was recrystallized in ethanol to afford the reddish purple needles (27 g, 98 % yield). ^{1}H-NMR (DMSO, δ ppm): 7.15 (dd, 2H), 7.34 (dd, 2H), 7.45 (dd, 2H), 7.86 (s, 4H). ESI-MS: *m/z* 239 $(M+H)^{+}$.

(2) **Synthesis of 1,8-Diaminoanthracene**

A solution of 1,8-diaminoanthraquinone (2.0 g, 8.4 mmol) in isopropanol (100 mL) was bubbled with nitrogen for 15 min before the introduction of sodium borohydride (4.0 g, 106 mmol). The resulting suspension was heated to reflux under nitrogen atmosphere for 60 min. After cooling to room temperature, the reaction mixture was poured into iced-water (250 mL). The dark green precipitates were filtered off and then washed thoroughly

with water. The solid was re-dissolved in chloroform (100 mL). The resulting solution was dried with anhydrous sodium sulfate. After removal of organic solvents with a rotary evaporator under reduced pressure, the product was purified by flash column chromatography (eluent: chloroform with 0 - 3 % methanol) to afford 1,8-diaminoanthracene (1.0 g, 55 % yield). ^{1}H-NMR ($CDCl_3$, δ ppm): 3.83 (br s, 4H), 6.76 (d, 2H), 7.30 (t, 2H), 7.48 (d, 2H), 8.35(s, 1H), 8.37 (s, 1H). ESI-MS: *m/z* 209 $(M+H)^+$.

(3) **Synthesis of 1,8-Bis(2,2-dipyridylamino) anthracene (BDPAA)**

A mixture of 2-bromopyridine (15 mmol, 1.5 ml), 1,8-diaminoanthracene (6 mmol, 1.25 g), $Pd_2(dba)_3$ (0.4 mmol, 16 mmol % Pd-cat, 180 mg), BINAP (0.4 mmol, 0.25 g) and *t*-BuONa (24 mmol, 2.4 g) was stirred at room temperature under argon for 5 min. A solution of 2-bromopyridine in toluene (1.0 ml of 2-bromopyridine in 45 ml toluene) was added drop-wise to the above mixture at room temperature. The resulting mixture was heated at reflux under argon for 10 h. After cooling to room temperature, the green precipitates were filtered off and washed thoroughly with acetone for several times. **BDPAA** (1.25 g, 40% yield) was obtained after dried in vacuum.. ^{1}H-NMR ($CDCl_3$, δ ppm): 6.68 (d, 4H), 6.74 (t, 4H), 7.31 (d, 4H), 7.47 (d, 2H), 7.53 (t, 2H), 8.04 (d, 2H), 8.19 (s, 4H), 8.38 (s, 1H), 8.60 (s, 1H). ESI-MS: *m/z* 518 $(M+H)^+$.

(4) **Synthesis of dinuclear [(Ru(*p*-cymene)Cl)$_2$BDPAA]Cl$_2$ complex**

A mixture of 300 mg of dichloro(*p*-cymene)ruthenium(II) (0.5 mmol) (*p*-cymene = 1-isopropyl-4-methylbenzene), 1.0 g of LiCl, 260 mg of **BDPAA** (0.5 mmol) were gently refluxed under nitrogen in 50 ml of dry THF for 2 h. After cooling to room temperature, the reaction solution was filtered to remove the insoluble matters. The filtrate was then concentrated to about 10 ml and yellow microcrystalline solids started to precipitate out from the solution. The solids were collected by filtration and washed thoroughly with

water and followed with diethyl ether. After drying in a vacuum oven, the dinuclear [(Ru(*p*-cymene)Cl)$_2$**BDPAA**]Cl$_2$ complex was obtained (0.45 g, 85% yield). Elemental analysis for $C_{54}H_{52}Cl_4N_6Ru_2$ Calcd.: C, 57.45; H, 4.64; N, 7.44. Found: C, 58.00; H, 4.71; N, 7.44; ESI-MS: $[M]^{2+}$ = 528.93.

(5) **Synthesis of mononuclear [Ru(*p*-cymene)(Cl)DPPA]Cl complex**

A mixture of 300 mg of dichloro(*p*-cymene)ruthenium(II) (0.5 mmol) (*p*-cymene = 1-isopropyl-4-methylbenzene), 250 mg of **DPPA** (*N*,*N*-di(2-pyridyl) phenylamine, 1.01 mmol) were gently heated to 100 °C in 50 ml toluene under nitrogen for 2 h. The mixture was then cooled to room temperature and the greenish yellow precipitates formed were collected by filtration. The solid was washed with acetone and followed with diethyl ether. After dried under vacuum, the complex of [**Ru(*p*-cymene)(Cl)DPPA]Cl** was obtained with 95 % yield. ESI-MS: $[M]^+$ = 517.84. ^{1}H-NMR (DMSO, δ ppm): 8.76 (2H, d, *J* = 6 Hz), 7.95 (2H, t, *J* = 6 Hz), 7.72 – 7.78 (4H, m), 7.60-7.70 (1H, m), 7.40 (2H, t, *J* = 7 Hz), 7.00 (2H, d, *J* = 7 Hz), 5.97 (2H, d, *J* = 6 Hz), 5.75 (2H, d, *J* = 6 Hz), 1.78 (3H, s), 1.19 (6H, d, *J* = 7 Hz).

(6) **General procedures for removal of chloro ligands from the Ru-complexes**

To a 25-ml round bottom flask the Ru-complex (0.5 mmol), AgOTf (20 mmol, 514 mg), and methanol (5 ml) were added. The mixture was stirred for 1 h under room temperature conditions. The silver chloride precipitates were filtered off and the organic solvent of the solution was removed under vacuum. The resulting solid was washed with de-ionized water and then diethyl ether. The greenish yellow powder was obtained after drying under vacuum at 40 °C for 24 h. The complex was characterized by ESI-MS with methanol as a solvent (Figure S4 and S5).

(7) General procedures for Ru-catalyzed addition of carboxylic acid to phenylacetylene

To a 25-ml round bottom flask the Ru-complex (0.04 mmol), phenylacetylene (1 mmol), acetic acid (1.2 equivalents, 80 ul), and 2.5 ml dry toluene were added. The reaction mixture was stirred and heated to 85 - 90 °C (oil bath temperature) under nitrogen atmosphere. After reaction for 24 h, the reaction mixture was cooled to room temperature and D.I. water (10 ml) was added. The aqueous solution was extracted with diethyl ether (10 ml for 3 times). The organic layers were collected and dried with anhydrous magnesium sulfate. After removal of organic solvents, the crude product of enol esters was purified by flash column chromatography (petroleum ether/ethylacetate = 20: 1) and then analyzed by GCMS.

(8) **TableS1.** The X-ray crystal structure (CCDC 899405), selected bond lengths, and bond angles for the dinuclear complex: [(Ru(*p*-cymene)Cl)$_2$**BDPAA**](CF$_3$SO$_3$)$_2$

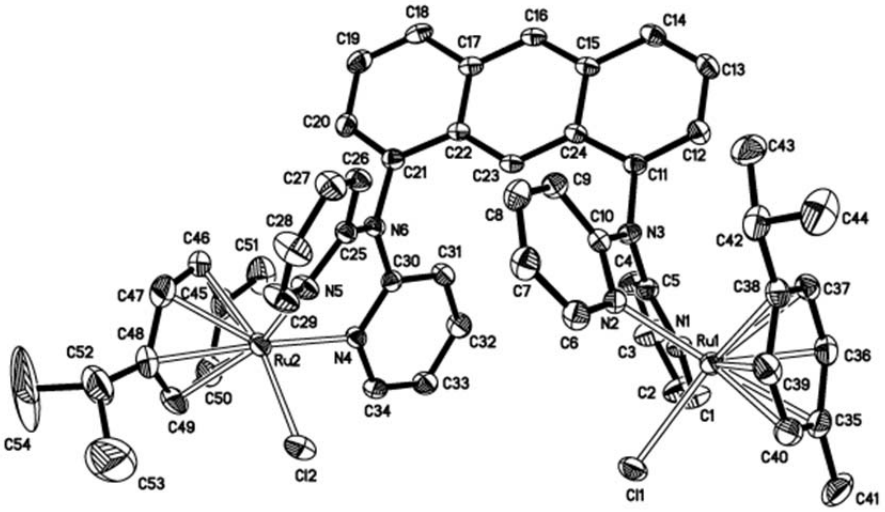

Bond length	(Å)	Bond angle	(°)
Ru(1)-N(1)	2.0965(14)	N(1)-Ru(1)-N(2)	82.95(5)
Ru(1)-N(2)	2.1029(14)	N(4)-Ru(2)-N(5)	81.99(6)
Ru(2)-N(4)	2.0803(14)	N(1)-Ru(1)-Cl(1)	84.55(4)
Ru(2)-N(5)	2.0874(15)	N(2)-Ru(1)-Cl(1)	87.02(4)
Ru(1)-Cl(1)	2.3953(5)	N(4)-Ru(2)-Cl(2)	86.44(4)
Ru(2)-Cl(2)	2.4064(6)	N(5)-Ru(2)-Cl(2)	86.64(5)

(9) **Table S2**. The *X*-ray crystal structure (CCDC 899406), selected bond lengths and bond angles for the mononuclear complex: [(Ru(*p*-cymene)Cl)**DPPA**]Cl

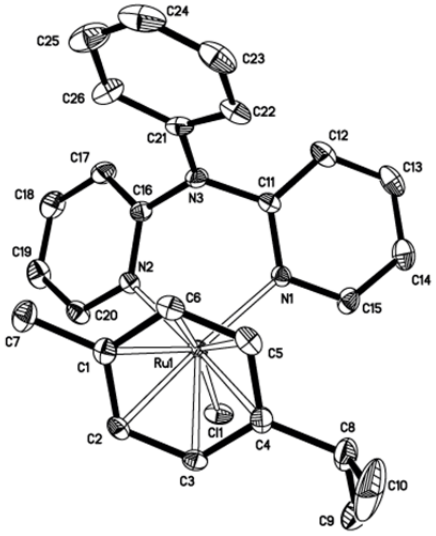

Bond length	(Å)	Bond angle	(°)
Ru(1)-N(1)	2.1170(19)	N(1)-Ru(1)-N(2)	83.30(8)
Ru(1)-N(2)	2.111(2)	N(1)-Ru(1)-Cl(1)	85.92(5)
Ru(1)-Cl(1)	2.4022(6)	N(2)-Ru(1)-Cl(1)	85.20(6)

(10) **Table S3.** Crystal and structure refinement data for the dinuclear complex: [(Ru(*p*-cymene)Cl)$_2$**BDPAA**](CF$_3$SO$_3$)$_2$

Empirical formula	$Ru_2Cl_2(C_{54}H_{52}N_6)\cdot CH_3CN\cdot (CF_3SO_3)_2$
Formula weight	1397.25
Temperature	296(2) K
Wavelength	0.71073 Å
Crystal system	Monoclinic
Space group	P2(1)/c
Unit cell dimensions	a=16.2205(2) Å, b=14.5792(2) Å, c=25.0080(3) Å α = 90°, β = 95.4810(10)°, γ = 90°.
Volume	5886.90(13) Å^3
Z	4
Density (calculated)	1.577 Mg/m^3
Absorption coefficient	0.750 mm^{-1}
F(000)	2832
Crystal size	0.36 x 0.34 x 0.30 mm^3
Theta range for data collection	1.62 to 27.37°.
Index ranges	-19<=h<=20, -18<=k<=18, -30<=l<=32
Reflections collected	50320
Independent reflections	13291 [R(int) = 0.0488]
Completeness to theta = 27.37°	99.6 %
Absorption correction	Multi scan
Max. and min. transmission	1.000 and 0.700
Refinement method	Full-matrix least-squares on F^2
Data / restraints / parameters	13291 / 51 / 811
Goodness-of-fit on F^2	1.01
Final R indices [I>2sigma(I)]	R_1 = 0.0550, wR_2 = 0.1520
R indices (all data)	R_1 = 0.0884, wR_2 = 0.1699
Largest diff. peak and hole	0.939 and -0.740 e.Å^{-3}

(11) **Table S4.** Crystal and structure refinement data for the mononuclear complex: [(Ru(*p*-cymene)Cl)**DPPA**]Cl

Empirical formula	$[RuCl(C_{26}H_{27}N_3)]\ Cl \cdot (H_2O)_{1.5}$
Formula weight	580.50
Temperature	296(2) K
Wavelength	0.71073 Å
Crystal system	Monoclinic
Space group	C2/c
Unit cell dimensions	a=17.8467(3) Å, b=19.9586(4) Å, c=14.4679(3) Å α = 90°, β = 93.8880(10)°, γ = 90°
Volume	5141.53(17) $Å^3$
Z	8
Density (calculated)	1.500 Mg/m^3
Absorption coefficient	0.844 mm^{-1}
F(000)	2376
Crystal size	0.48 x 0.20 x 0.16 mm^3
θ range for data collection	1.53 to 27.47°.
Index ranges	-23<=h<=23, -25<=k<=25, -18<=l<=17
Reflections collected	40721
Independent reflections	5888 [R(int) = 0.0572]
Completeness to θ = 27.47°	99.9 %
Absorption correction	Semi-empirical from equivalents
Max. and min. transmission	0.7456 and 0.5578
Refinement method	Full-matrix least-squares on F^2
Data / restraints / parameters	5888 / 0 / 381
Goodness-of-fit on F^2	1.004
Final R indices [I>2sigma(I)]	R_1 = 0.0389, wR_2 = 0.1150
R indices (all data)	R_1 = 0.0488, wR_2 = 0.1300
Largest diff. peak and hole	0.916 and -0.761 $e.Å^{-3}$

(12) **Figure S1**. Possible mechanisms involved in addition of acetic acid to phenylacetylene.

(A) Possible reaction pathway for E-enol ester formation:

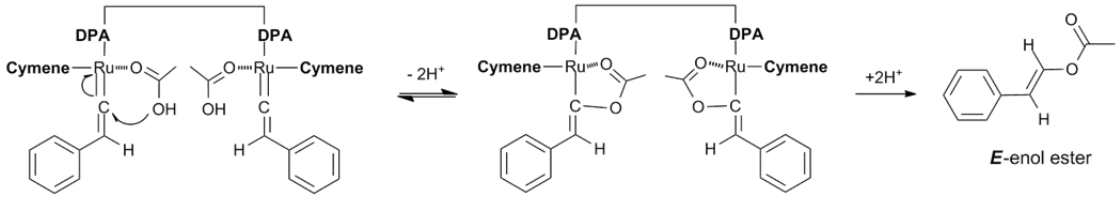

(B) Possible reaction pathway for Z/E-enol esters formation:

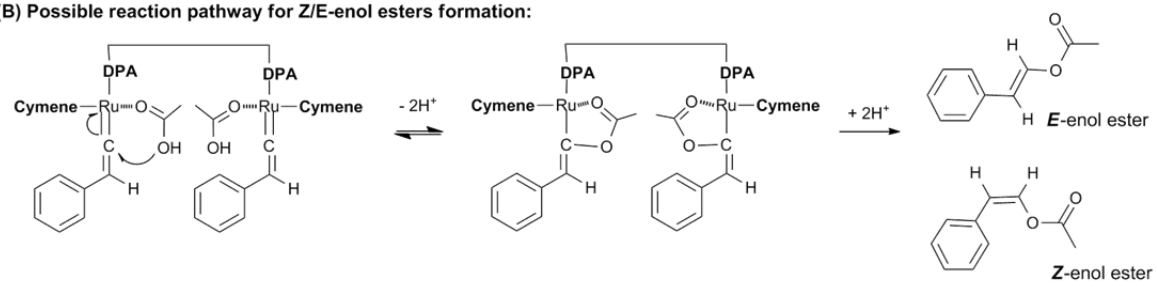

(C) Possible reaction pathway for Z-enol ester formation:

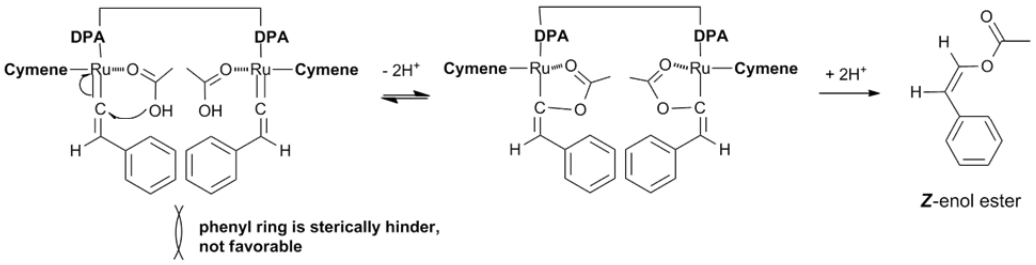

(D) Possible reaction pathway for the formation of Z- and E-enol ester catalyzed by the mononuclear Ru-complex:

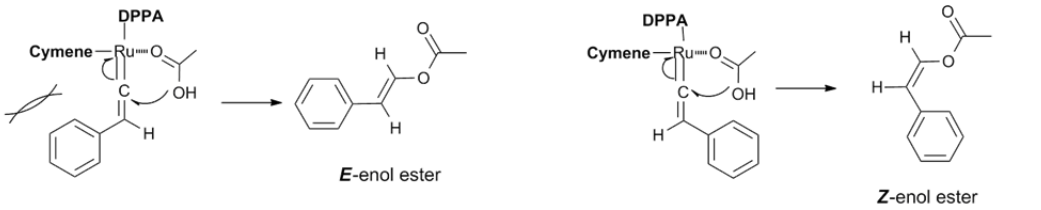

phenyl ring is sterically hinder as it is close to the cymene group, less favorable

less steric strain, more favorable
This is the reason why mononuclear Ru-complex produces Z-enol ester dominantly in the catalysis though its stereoselectivity is very not high

Ligands:

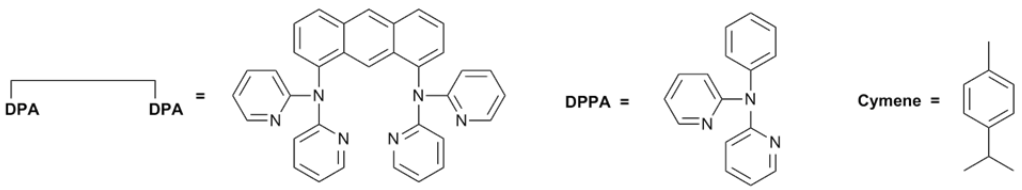

(13) **Figure S2**. ESI-MS of the dinuclear complex: [(Ru(*p*-cymene)Cl)$_2$ **BDPAA**](CF$_3$SO$_3$)$_2$

(A) Experimental data:

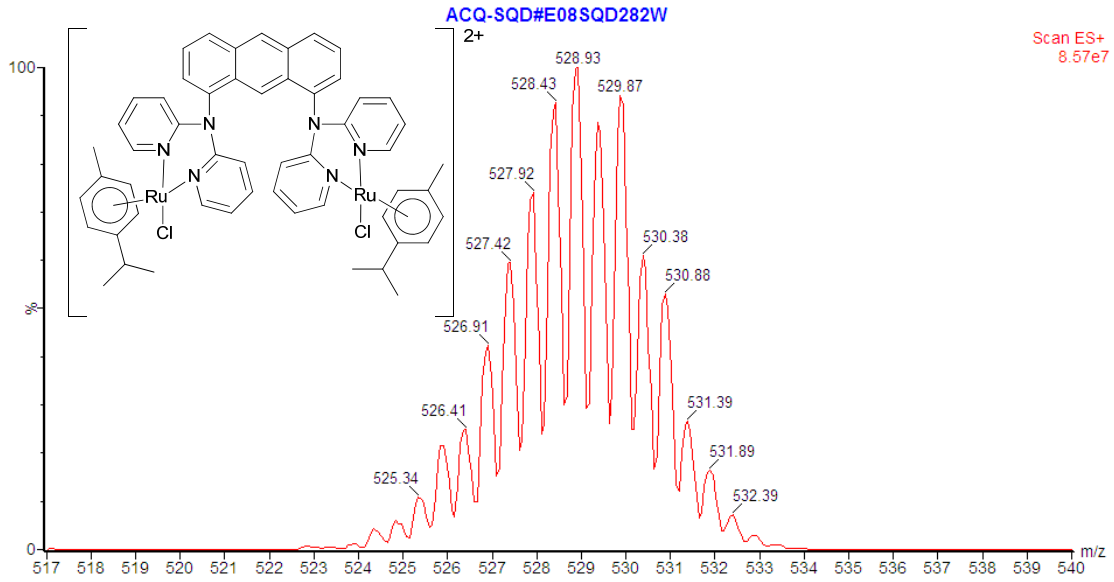

(B) Simulated spectrum (isotopic distribution graph) for the dinuclear complex: [(Ru(*p*-cymene)Cl)$_2$**BDPAA**](CF$_3$SO$_3$)$_2$

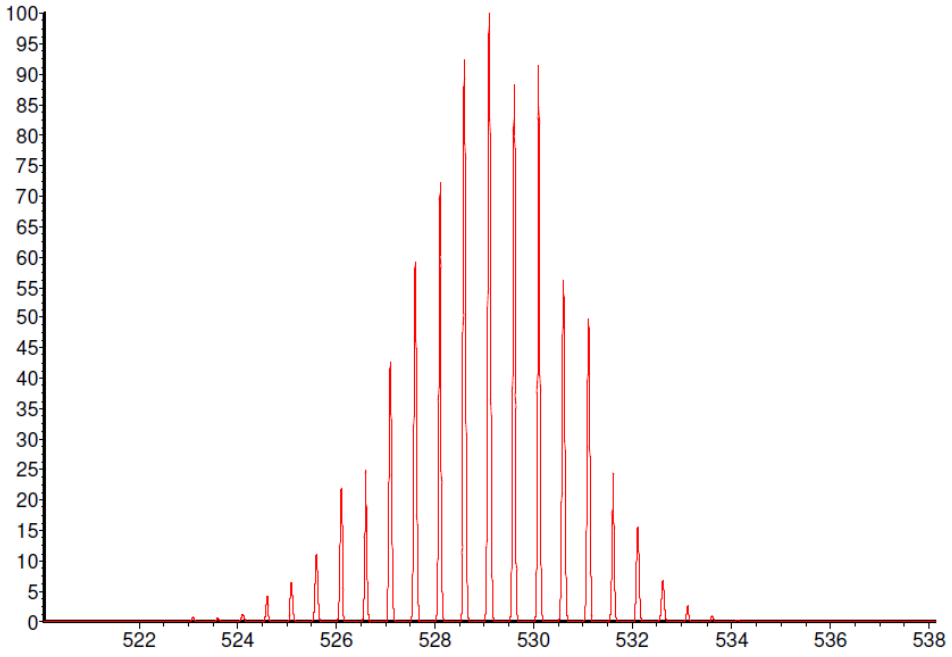

(14) **Figure S3**. ESI-MS of the mononuclear complex: [(Ru(*p*-cymene)Cl)**DPPA**]Cl

(A) Experimental data:

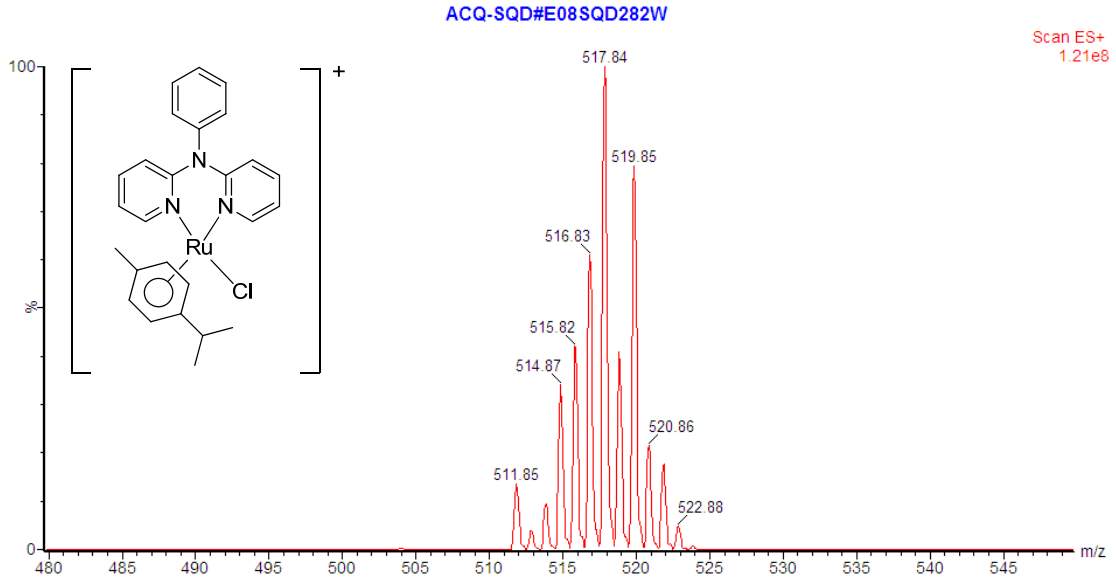

(B) Simulated spectrum (isotopic distribution graph) for the mononuclear complex: [(Ru(*p*-cymene)Cl)**DPPA**]Cl

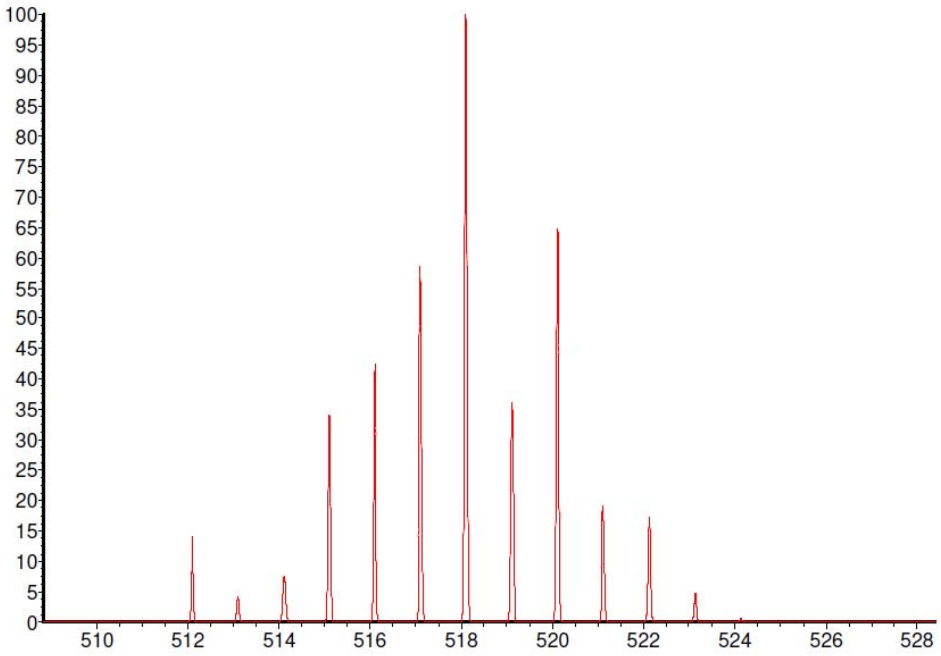

(15) **Figure S4**. ESI-MS of the active mononuclear catalyst [(Ru(*p*-cymene)](CF_3SO_3)**DPPA**](CF_3SO_3) after removal of the chloride ligand with Ag^+

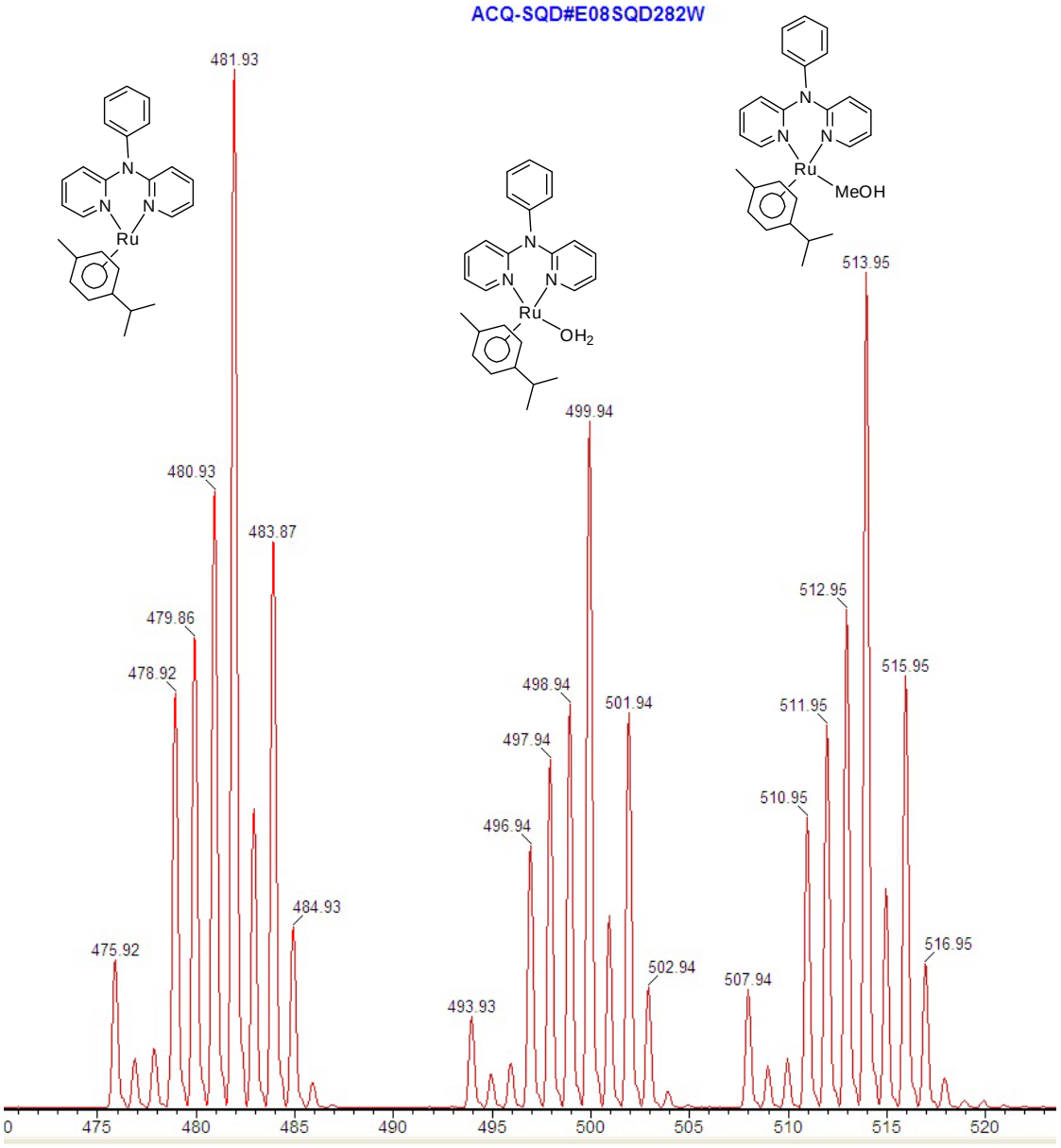

(16) **Figure S5**. ESI-MS of the active dinuclear catalyst [(Ru(*p*-cymene)(CF_3SO_3))$_2$ **BDPAA**](CF_3SO_3)$_2$ after removal of the chloride ligands by Ag^+

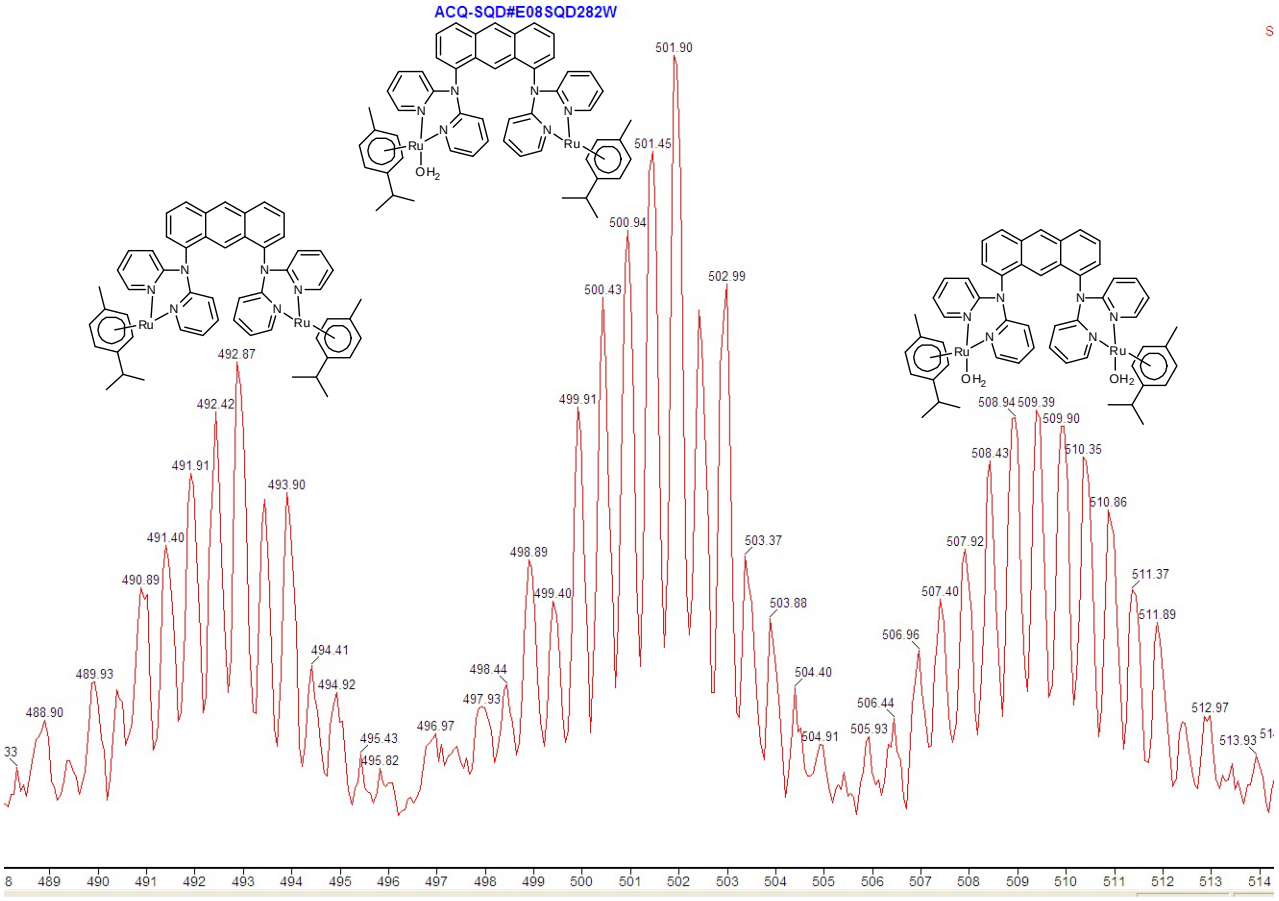

(17) **Figure S6**. ^{13}C NMR Spectrum of a reaction of mononuclear catalyst [(Ru(*p*-cymene)](CF_3SO_3)**DPPA**](CF_3SO_3) with phenylacetylene in CD_3OD.

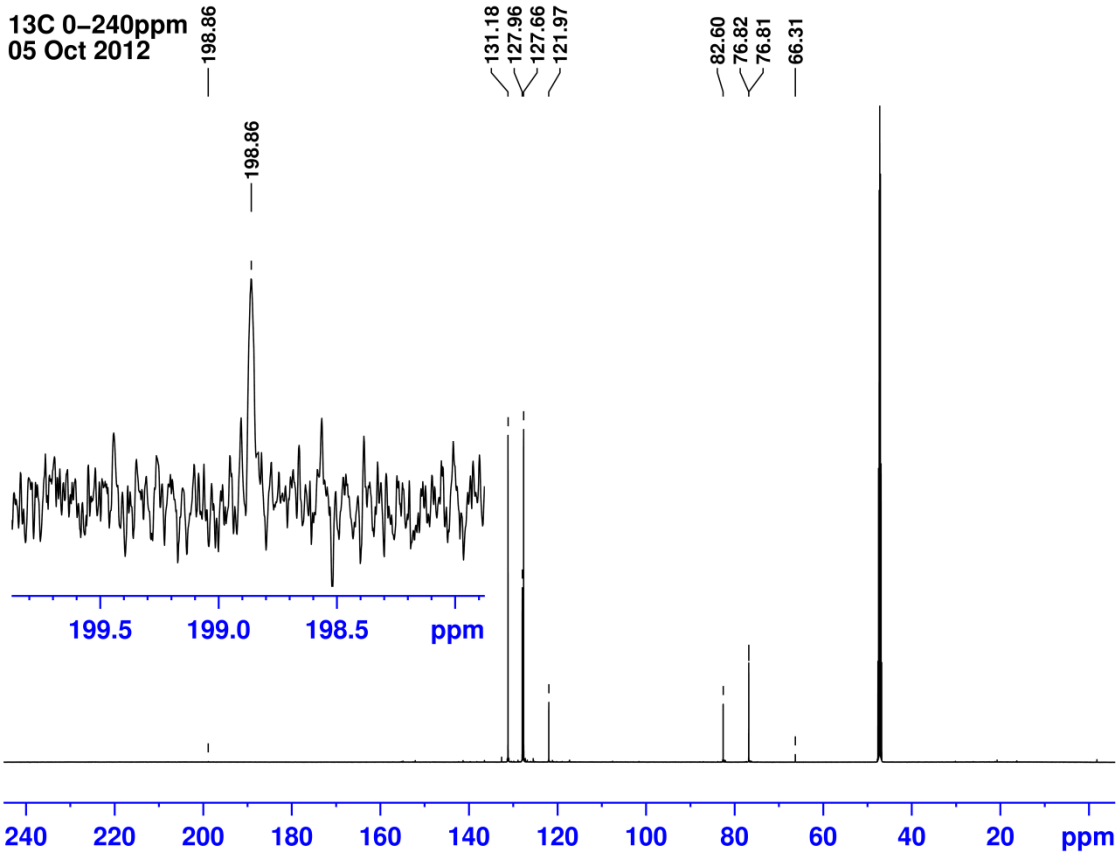

(18) **Figure S7**. ^{13}C NMR Spectrum of a reaction of dinuclear catalyst [(Ru(*p*-cymene)$(CF_3SO_3))_2$ **BDPAA**]$(CF_3SO_3)_2$ with phenylacetylene in CD_3OD.

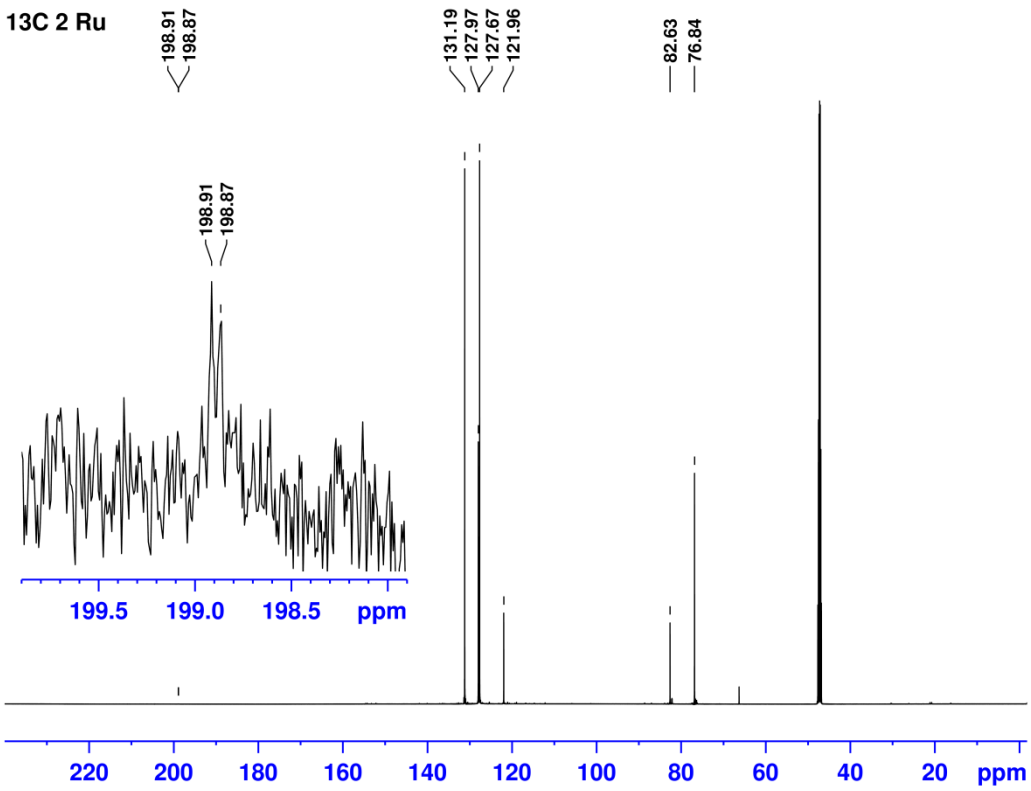

(19) **Figure S8**. ESI-MS of the reaction of active mononuclear catalyst [(Ru(*p*-cymene)](CF_3SO_3)**DPPA**](CF_3SO_3) with phenylacetylene.

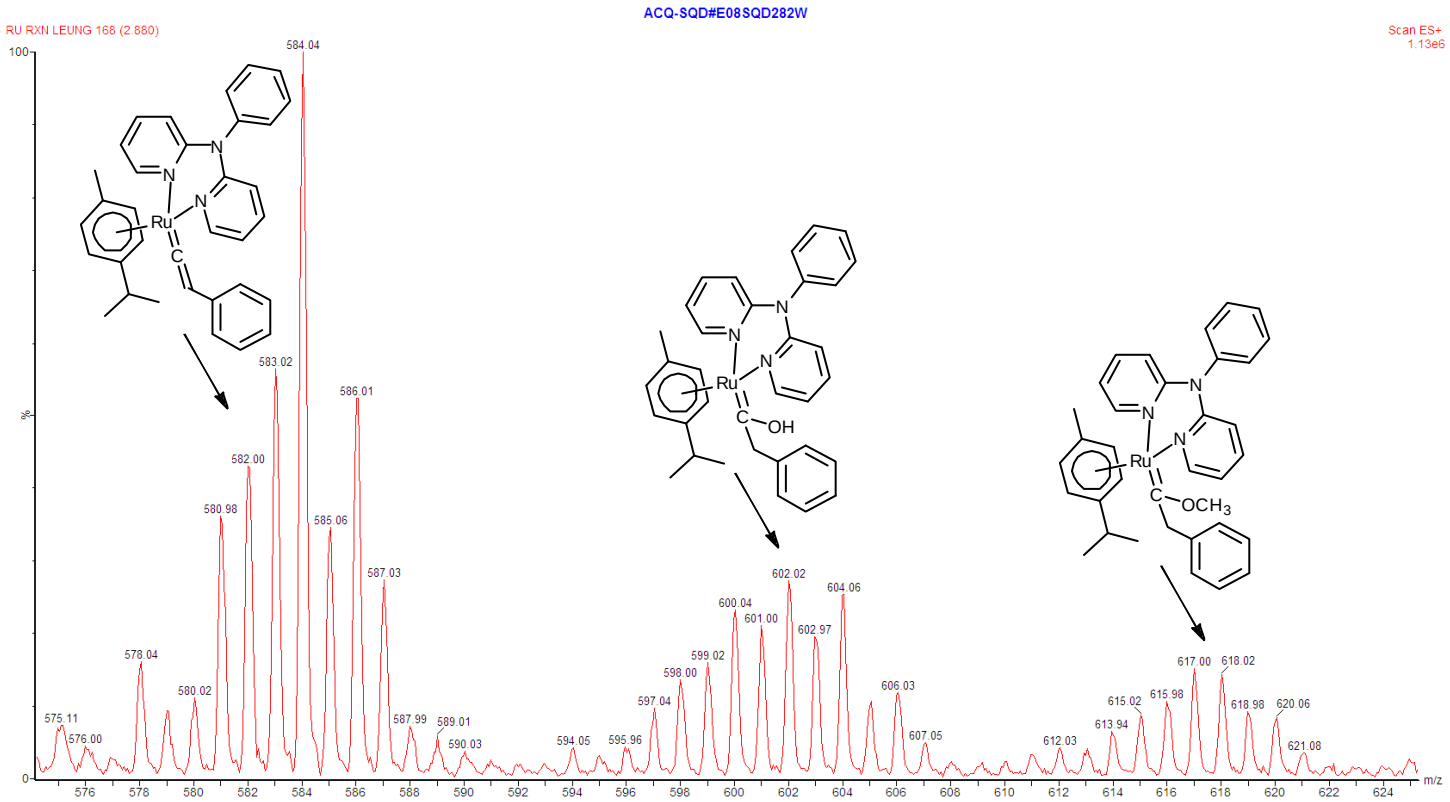

(20) **Figure S9**. ESI-MS of the reaction of active dinuclear catalyst [(Ru(*p*-cymene)(CF_3SO_3))$_2$ **BDPAA**](CF_3SO_3)$_2$ with phenylacetylene.